GeoHealth

RESEARCH ARTICLES

10.1029/2022GH000607

Key Points:

- Water discharge homogenization and sediment concentration reduction were found in the Three Gorges Reservoir inflows during 2007–2016
- Ammonia nitrogen and total nitrogen concentrations are insensitive to changed water and sediment inflows
- N_2 emission varied violently, presenting quick response under changed hydrological conditions

Supporting Information:

Supporting Information may be found in the online version of this article.

Correspondence to:

Y. Yue,
yueyao@whu.edu.cn

Citation:

Pang, L., Sun, Y., Yue, Y., Liu, C., An, C., Yang, T., et al. (2022). Stability of aquatic nitrogen cycle under dramatic changes of water and sediment inflows to the Three Gorges Reservoir. *GeoHealth*, *6*, e2022GH000607. https://doi.org/10.1029/2022GH000607

Received 14 FEB 2022
Accepted 21 JUL 2022

Stability of Aquatic Nitrogen Cycle Under Dramatic Changes of Water and Sediment Inflows to the Three Gorges Reservoir

Lina Pang[1,2], Yanxin Sun[1], Yao Yue[1], Caiqiong Liu[1], Chenge An[3], Tiantian Yang[1], Xinhua Lu[1], Quanxi Xu[4], Jie Mei[1], Min Liu[5], and Xiaofeng Zhang[1]

[1]State Key Laboratory of Water Resources and Hydropower Engineering Science, School of Water Resources and Hydropower Engineering, Wuhan University, Wuhan, China, [2]College of Architecture and Environment, Sichuan University, Chengdu, China, [3]Department of Hydraulic Engineering, State Key Laboratory of Hydroscience and Engineering, Tsinghua University, Beijing, China, [4]Bureau of Hydrology, Changjiang Water Resources Commission, Wuhan, China, [5]Wenhua College, Wuhan, China

Abstract Stability of nitrogen cycle is a key indicator to aquatic health. In recent years, water and sediment inflows to the Three Gorges Reservoir (TGR) have changed significantly. To reveal the effects of such dramatic hydrological changes on aquatic nitrogen cycle, this paper at first analyzed the changing trends of water and suspended sediment discharges of TGR based on dynamic harmonic regression, and found that the intra-year distribution of water flow was significantly homogenized between flood and dry seasons, with the seasonal variations narrowed by 43.5%–69.9% during 2007–2016, while sediment concentration sharply dropped (the non-periodic term decreased by 1.48%–2.07%/month). Modified with the effects of sediment concentration variations on nitrification/denitrification rates, the proposed numerical model surprisingly showed that ammonia nitrogen and total nitrogen concentrations in TGR were insensitive to either water flow homogenization or sediment reduction, implying relative stability of microbial community related to nitrogen cycle, which is a positive sign for aquatic health. However, N_2 emission varied more violently. The variation range of nitrogen gas (N_2) emitted from TGR enlarged by 30% with the homogenization of water inflow from 2010 to 2016, while the annual total N_2 emission decreased by 7% due to the reduction of sediment concentration, indicating quick response and strong adaption of the microbial N_2 producing process to the environmental changes of TGR, which is beneficial for maintaining ecological functions related to nitrogen cycling. This work helps understanding nitrogen cycle of reservoirs experiencing dramatic changes in water and sediment inflows.

Plain Language Summary Nitrogen cycle is a global issue related to environmental health. The hydrological conditions of water bodies are responsible for water health with nitrogenous substances as indicators. Considering the significantly changed water and sediment inflows to the Three Gorges Reservoir (TGR), the effects of such dramatic hydrological changes on nitrogen cycle were revealed. We developed a numerical model, modified with the effects of sediment concentration variations on nitrogen cycle, to estimate the response of nitrogenous substances to the changed hydrological conditions. The insensitive ammonia nitrogen and total nitrogen concentrations were obtained to either the flattened annual water flow process or the sharply reduced sediment concentration in the inflows to the TGR, implying relative stability of microbial community related to nitrogen cycle, which is a positive sign for aquatic health. In contrast, N_2 emission was very sensitive, indicating quick response and strong adaption of the microbial N_2 producing process to the environmental changes of TGR, which is good for maintaining ecological functions related to nitrogen cycling. Findings of this work are useful for understanding nitrogen cycle of reservoirs experiencing dramatic changes in water and sediment inflows which have occurred globally.

1. Introduction

Nitrogen cycle in ecosystems, primarily consisting of ammonification, nitrification, and denitrification, is a fundamental process that actively affects environmental health. Emission of nitrous oxide gas (N_2O) during denitrification induces not only warming effect, but also harmful ultraviolet radiation (Quick et al., 2019). Accumulation of ammonia nitrogen and nitrate nitrogen in lakes or reservoirs results in eutrophication, deteriorating water quality and reducing biodiversity, and finally impairing aquatic environmental health (Wang et al., 2010). Recent studies indicated that nitrogen cycle, mainly driven by microbial processes (Knoll et al., 2012), is strongly

influenced by the hydrological conditions of water bodies (Wang et al., 2010; Xia et al., 2017; Yu et al., 2019). Since the stability of nitrogen cycle is a key indicator to aquatic health (Reaver et al., 2021), linking the nitrogenous substances in nitrogen cycling with hydrological variations have been concerns of many studies for the environmental health of water bodies in different forms (Abdul-Aziz & Ahmed, 2017; Schrag, 2017), especially considering that substantial changes in discharge and sediment transport have widely occurred in global rivers (Chai et al., 2020; Li et al., 2020).

As the largest hydropower project in the world, the Three Gorges Reservoir (TGR), located at the main channel of the Yangtze River, keeps attracting intensive attention to its aquatic environmental health, especially in the perspective of nitrogen concentration variations (Tong et al., 2017). In the meantime, dramatic changes in water and suspended sediment inflows have occurred due to the impoundment of its upstream cascade reservoirs, soil conservation in the upper Yangtze River Basin, and climate change. Chai et al. (2020) found that allocation of water discharge between dry and flood seasons had been homogenized along the entire reach of the Yangtze River. Zhang et al. (2019) revealed that the annual sediment in the Jinshajiang Reach (the upper-most reach of the Yangtze River) had decreased sharply since 2010, leading to reduction of sediment inflow into the TGR. Such radical changes in hydrological conditions of the TGR obviously alter aquatic nitrogen cycle through microbial processes. For instance, the homogenized inflow may affect river ecosystems, including the diversity and composition of microbial community related to the nitrogen cycle by changing the concentration of suspended particulates and nitrogenous matters, both of which have tight relationships with microorganisms driving nitrification and denitrification processes (Widdig et al., 2020; Xia et al., 2017; Zhang et al., 2021). Besides, the ammonification and nitrification processes on sediment surface are also affected by water and sediment conditions (Liu et al., 2021; Yu et al., 2016), with profound implications for the stability of nitrogen cycle, and thus, the aquatic environmental health.

As a classic tool in characterizing profiles of nitrogen transportation and transformation in waters, numerical model of aquatic nitrogen cycle has been applied to analyze the impacts of short-term variations of water conditions (e.g., flow velocity, water level, etc.) on nitrification and denitrification processes (Gu, 2005; Yu et al., 2019). However, the influence of long-term trend in water flow has not been discussed. As to the variations in suspended sediment, lab-scale studies have been carried out to investigate relationships between suspended sediment concentration and the reaction rates of nitrification, denitrification, and/or ammonia oxidation (Wang et al., 2010; Xia et al., 2017). However, the linkage of the sediment concentration change with the nitrogen cycle in natural waters still need to be analyzed with the help of numerical models.

This paper aims to analyze how the changes in water and sediment inflows in TGR would affect the stability of aquatic nitrogen cycle with indicators of the variations in ammonia nitrogen (NH_3-N), total nitrogen (TN) and nitrogen gas (N_2) during a relatively long period (2007–2016). Therefore, the annual and intra-year changing trends of water discharge and sediment concentration have been at first investigated using dynamic harmonic regression (DHR) method which divides time series into the periodic and non-periodic items. Then, an aquatic nitrogen cycle model incorporating the effects of suspended sediment concentration change on the biochemical reaction rates of nitrification/denitrification has been set up to simulate the process that NH_3-N and TN concentrations and N_2 emission change with water and sediment inflow variations. Finally, implications for the stability and adaption of microbial communities involving in main nitrogen cycle processes have been discussed. Observations of water flow, suspended sediment, NH_3-N, TN, and pH, were collected at the upstream entrance of the TGR (the Qingxichang Station) and the middle of the reservoir area (the Wanxian Station) to calibrate and validate the numerical model, as well as to drive the DHR method. This study provides insights into how the changes in water and sediment inflows in TGR would affect the stability of aquatic nitrogen cycle.

2. Study Area and Data Collection

The study area is the reach of the Yangtze River mainstream ranging from Qingxichang Station (QXC) to Wanxian Station (WX), with a total length of about 190 km. Considered as a typical reservoir area of the TGR, it flows through Fuling District, Fengdu County, Zhongxian County and Wanzhou District in Chongqing, China (Figure 1).

All data used in this study was from the Bureau of Hydrology, Changjiang Water Resources Commission, and measurements of physical and chemical data were conducted according to standard methods (APHA et al., 2012;

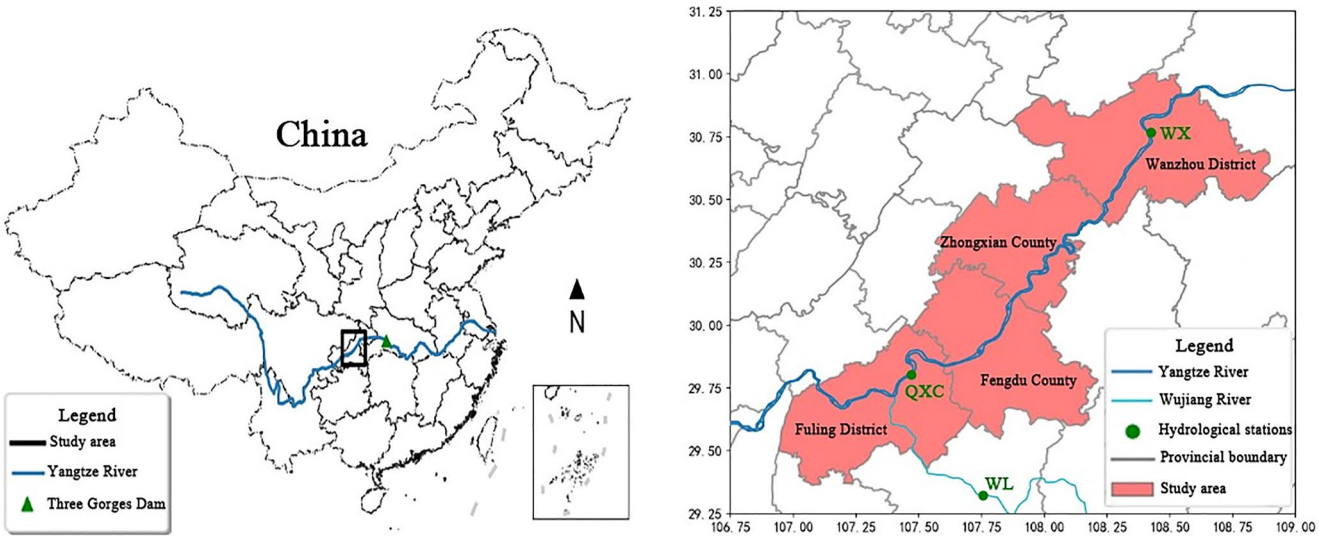

Figure 1. Study area of the Three Gorges Reservoir and hydrological stations.

HJ535-2009, 2009). According to the Regulation for Water Environmental Monitoring (SL219-2013, 2013), three perpendiculars were set at the midstream, near the left bank and the right bank of QXC and WX, respectively, with three sampling points selected at 0.5 m underwater, 0.5 m above bottom and half depth, respectively, because the widths of QXC and WX sections are between 100 and 1,000 m and the depths are over 10 m. Then, the NH_3-N and TN were computed as the simple average over the nine points. Surface floating materials were avoided when sampling. All samples precipitated naturally for 30 min to filter out solids. According to the Environmental Quality Standards for Surface Water (GB3838-2002, 2002), samples after precipitation should be further filtered through 0.45 μm polycarbonate membrane filters if obviously polluted. Then, the supernatant liquid/filtrate was acidified by sulfuric acid and frozen at −20°C until analysis. NH_3-N was determined by Nessler's reagent spectrophotometry through generation of yellowish brown colloidal compounds (HJ535-2009, 2009), and TN was analyzed using method of alkaline potassium persulfate digestion-ultraviolet spectrophotometry through oxidative digestion of all digestible nitrogen forms to nitrate, followed by quantitation of the nitrate (APHA et al., 2012), and there was no detection of intermediates from NH_3-N through N_2 (e.g., nitrite). For establishing the hydrodynamic and nitrogen models, daily data of water level and flow quantity and monthly data of NH_3-N and TN were collected from 2010 to 2011 and in 2016. Water, sediment, and nitrogen data from 2010 to 2011 were used for calibration (data of 2010) and validation (data of 2011). Model results based on data of 2010 and 2016 were compared to analyze the effects of homogenized water flow and reduced sediment concentration. Besides, monthly data of water discharge and sediment concentration from 2007 to 2016 were used to drive the DHR method. According to the Bureau of Hydrology, Changjiang Water Resources Commission, monitoring methods and instrument detection limit could bring in uncertainty of less than 5%. Time series data of water flow, suspended sediment concentration, NH_3-N and TN concentrations at QXC and WX stations were shown at https://doi.org/10.5281/zenodo.6801085 (Yue, 2022).

3. Methods

3.1. DHR Analysis

Dynamic Harmonic Regression (DHR) method was carried out to quantify the annual and seasonal changes of water discharge, suspended sediment concentration, and concentrations of NH_3-N and TN, by dividing time series into the trend term (non-periodic) and the periodic term, as given in Equation 1.

$$y_t = T_t + C_t + S_t + e_t \quad (1)$$

where y_t is the measured data series, T_t is the trend term, C_t is the periodic term of high frequency, S_t is the seasonal term, and e_t is the predicted residual. S_t and C_t are determined by Equation 2.

$$C_t + S_t = \sum_{i=1}^{N/2} \left[a_{i,t} \cos(\omega_i t) + b_{i,t} \sin(\omega_i t) \right] \tag{2}$$

in which N is the number of the longest period in monitoring (e.g., $N = 12$ when monthly data is studied); $a_{i,t}$ and $b_{i,t}$ are the coefficients which are to be determined to achieve best fitness between the regression and the studied series; ω_i is harmonic frequency; t is the time. Taylor et al. (2007) is referred to for the estimation of ω_i and the determination coefficient R^2 which shows the fitness of the DHR series into observations. In this study, trend coefficient δ_T and seasonal coefficient δ_S, showing the interannual trend and seasonal amplitude change of discharge and sediment series, are defined by Equations 3 and 4, respectively.

$$\delta_T = \frac{\Delta T_i}{\Delta t} \cdot \frac{1}{\bar{\hat{y}}} \tag{3}$$

$$\delta_S = \frac{S_{t\max} - S_{t\min}}{\hat{y}_{t\max} - \hat{y}_{t\min}} \tag{4}$$

where ΔT_t is the increment of trend term over Δt (time duration, 1 month in this study); $\bar{\hat{y}}$ is the perennial mean value of fitted data in the studied period; δ_T is the variation rate of trend term; S_{tmax} and S_{tmin} are the maximum and minimum values of seasonal term in 1 year, respectively; $\hat{y}_{t\max}$ and $\hat{y}_{t\min}$ are the maximum and minimum values of fitted data, respectively; δ_S presents the variability of seasonal term.

3.2. One-Dimensional Water Flow and Suspended Sediment Transport Model

The one-dimensional model has been widely applied and validated applicable to simulate the hydrodynamics and morphodynamics of large low-land rivers, such as the Yangtze River (Guo et al., 2016), the Yellow River (An et al., 2018), the Mississippi River (Nittrouer & Viparelli, 2014), the Rhine River (Ylla Arbós et al., 2021), and many other rivers worldwide, especially at relatively long temporal and spatial scales. Here, we proposed a one-dimensional water flow and suspended sediment transport model which is reasonable when the focus is the temporal variation and longitudinal (i.e., cross sectional averaged) distribution of sediment concentration. A more complex model with consideration of multi-dimensionality, though not being the focus of this paper, would surely merit future research.

The one-dimensional open channel unsteady flow model (Equation 5) and the one-dimensional unsteady unsaturated suspended sediment transport model (Equation 6) were employed for calculating hydrodynamic conditions and the distribution of suspended sediment across the studied area.

$$\begin{cases} B\dfrac{\partial Z}{\partial t} + \dfrac{\partial Q}{\partial x} = 0 \\ \dfrac{\partial Q}{\partial t} + \left(gA - \dfrac{BQ^2}{A^2} \right) \dfrac{\partial Z}{\partial x} + 2\dfrac{Q}{A}\dfrac{\partial Q}{\partial x} = \dfrac{Q^2}{A^2}\dfrac{\partial A}{\partial x}\bigg|_Z - gn^2 \dfrac{|Q|Q}{AR^{4/3}} \end{cases} \tag{5}$$

$$\frac{\partial}{\partial t}(\mathrm{AS}) + \frac{\partial}{\partial x}(\mathrm{QS}) = -\alpha B \omega (S - S_*) \tag{6}$$

in which B is the width of water surface (m); Z is water level (m), Q is water discharge (m^3/s); t is time (s); x is the distance from the start section of the channel along the direction of flow (m); A is the area of cross-section (m^2); g is the gravitational acceleration (m/s^2); n is the Manning's roughness; R is the hydraulic radius (m, as the ratio of river width to water depth is very large, here we used water depth to approximate R); S is suspended sediment concentration (kg/m^3); S_* is suspended sediment transport capacity (kg/m^3) derived from the Zhang (1998)'s formula; α is sediment recovery saturation coefficient and set to be 0.25, and ω is the suspended sediment settling velocity (m/s) (Zhang, 1998).

To solve the flow model, we used the four-point implicit Preissmann scheme. For model stability, the weighting factor should be larger than 0.5. Here 0.7 was set following Liu et al. (1994). For solving the suspended sediment transport equation, the forward-differencing scheme was used for the time-derivative term, and the upwind scheme was used for the convection term. Ninety-three cross sections with average intervals of 2081.4 m were divided from QXC to WX. The initial water flow conditions of the studied reach were calculated by assuming a

steady flow condition, while the initial suspended sediment concentration of every cross-section was obtained by linear interpolation between QXC and WX according to the distance of each section to the dam. Time-varied discharge and suspended sediment concentration were prescribed at QXC and water level is prescribed at WX.

3.3. One-Dimensional Model of Aquatic Nitrogen Cycle Modified With Sediment Variations

A one-dimensional model which incorporates aquatic nitrogen cycle with the processes of hydrodynamics and morphodynamics was proposed to obtain a first-order understanding of the effect of changes in water and sediment inflows on the aquatic nitrogen cycling. We should notice that pools of NH_3-N and TN are coupled. NH_3-N is first nitrified into NO_3-N, then NO_3-N is denitrified into N_2 or other nitrogenous gases. There may be some intermediate products like NO_2-N, but we assume the nitrification is a one-step reaction, and denitrification is another one-step reaction (i.e., no intermediate products like NO_2-N exist, and N_2 is the only end-point). Based on this assumption, we used two equations which have a similar form to simulate the variations of NH_3-N and TN concentrations, respectively (Equation 7):

$$\frac{\partial}{\partial \mathrm{t}}(\mathrm{AC}) = \frac{\partial}{\partial x}\left[\mathrm{AE}\frac{\partial C}{\partial x}\right] - \frac{\partial}{\partial x}(\mathrm{QC}) + \mathrm{AF}(C) + \Omega \tag{7}$$

in which A is the area of cross-section (m^2); C is the mean concentration of NH_3-N or TN at each cross section (mg/L); t is time (s); x is the distance from the start section of the channel along the direction of flow (m); E is the river longitudinal dispersion coefficient (m^2/s); Q is water discharge (m^3/s); $F(C)$ is the biochemical reaction term; Ω is the source/sink term.

When Equation 7 was used to simulate variations of NH_3-N concentration, the biochemical reaction term, $F(C)$, represents the one-step process that NH_3-N is nitrified into NO_3-N, and the first-order kinetic reaction was adopted, that is, $F(C) = -K_{\mathrm{NH3\text{-}N}}C$. Our improvement to simulate the nitrification process in this study was to take the influence of radical sediment reduction on biochemical reactions in natural waters into consideration. A modified equation (Equation 8) for suspended sediment concentration based on NH_3-N degradation coefficient given by Gu (2005) was applied in nitrification process modeling:

$$K_{\mathrm{NH_3-N}} = K_0\left(0.015 + 0.197 \times I^{0.599} \times \frac{u}{h}\right) \times 1.083^{T-20} \tag{8}$$

where $K_{NH3\text{-}N}$ is ammonia nitrogen degradation coefficient (1/d); I is river gradient; u is the average velocity of the cross section; h is the average depth of the cross section; T is water temperature (°C). The effect of suspended sediment concentration on nitrification is included in the baseline ammonia nitrogen degradation coefficient of K_0 as follows:

$$K_0 = p_1 \cdot S^{p_2} \tag{9}$$

where S is suspended sediment concentration. It should be noted that the form of Equation 9 was supported by the indoor experiments carried out by Xia et al. (2017). Considering the difference of reaction environments of indoor experiments and natural waters, we set two parameters, p_1 and p_2, to be determined by calibration in the ranges of 0–10 and 0–1.0.

When Equation 7 was used to simulate variations of TN concentration, we should notice that nitrification of NH_3-N does not change TN concentration. It only leads to the transformation of nitrogen from the NH_3-N form to the NO_3-N form. However, denitrification into nitrogenous gases does lead to losses of TN from the water body. Therefore, we only considered the nitrogenous gas emission process in the biological reaction term, $F(C)$. Here we assumed that all the NO_3^- were converted into N_2 in denitrification process, and TN loss through biochemical reactions was only resulted from N_2 gas emission from the water body. Uncertainty induced by this assumption is in the Discussion Section. The one-step first-order kinetic reaction was also adopted, and modified based on Xia et al. (2017) (Equation 10):

$$R_{N_2} = p_3 S^{0.0535} C_{NO_3-N}^{p_4} \tag{10}$$

in which R_{N2} is the emission rate of N_2; S is still the suspended sediment concentration; C_{NO_3-N} is nitrate nitrogen concentration (mg-N/L). Similarly, here we also set p_3 and p_4 as parameters to be determined by calibration in the

ranges of 0–10 and 0–1.0 to reflect the difference of indoor experiments by Xia et al. (2017) and natural waters. When the model was calibrated and successfully validated by the observed TN data series, the model can be used to simulate TN change under the impacts of discharge homogenization and sediment reduction.

We should also notice that dissolved N_2 and N_2 emission rates could not be accurately measured without ^{15}N tracers or $\delta^{15}N$ assays in indoor experiments. In this study, we tried to simulate variations of nitrogenous substances in a relatively long period in a natural water body, which limited the implementation of ^{15}N tracers or $\delta^{15}N$ assays method. Therefore, we calculated N_2 emission instead of measuring. Once p_3 and p_4 are determined through calibration, N_2 emission rates can be calculated using Equation 10 when S and $C_{NO3\text{-}N}$ are given by the suspended sediment transport model (Equation 6) and interpolation of the measured NO_3-N data, respectively.

In this study, Ω mainly includes the exogeneous loads from lateral flows (i.e., tributaries of the TGR, Zhao et al., 2019). No NH_3-N was assumed to emit from the sediment on the bottom of the bed into the overlying water, because the maximum NH_3-N emission from the bottom sediment observed at the Cuntan station on the Yangtze River was reported to be 0.602 mg/m^2/d (Xia et al., 2008), very small compared to the concentration of 4.480–5.423 mg/m^2 in the overlying water. To estimate the exogenous sources (i.e., Ω in Equation 7), we considered both the natural background loads in tributaries, and the loads due to pollution in the reservoir drainage area. The natural background loads in tributaries at impoundment water levels of 175 m, 155 m, and 145 m were given by Deng (2007) (Table S1 in Supporting Information S1). Thus, the natural background exogenous loads from lateral flows at other impoundment water levels of the TGR can be obtained by interpolation. After collecting the total pollution loads of NH_3-N and TN at three levels (i.e., low, medium, and high) from the whole reservoir area in 2010 and 2015 (Yu et al., 2010), the specific pollution loads from different tributaries were allocated by calculating the percentage of drainage area of the tributaries in each district or county along the reservoir (Table S2 in Supporting Information S1). The intra-year distribution of pollution loads among flood period (from June to September), normal period (from April to May, and from October to November), and dry period (from December to next March) was obtained through calibration based on genetic algorithm (Ran et al., 2017).

The discrete scheme adopted by Deng (2007) was also used here. The implicit scheme was used to discretize the change terms in the equation. The initial conditions at each section were prescribed through inverse-distance weighted interpolation of the measured data on the first day between QXC and WX stations. At the upper boundary, observed NH_3-N and TN data at the QXC station was prescribed, while at the lower boundary a transmitting boundary condition was used (Deng, 2007).

4. Results

4.1. Annual and Intra-Year Changing Trends of Water and Sediment Inflows

Good fittings of flow and suspended sediment concentration series at QXC and WX stations were derived by DHR (Figure S1 in Supporting Information S1). The annual trend terms in Figures 2a and 2b illustrated that water discharge did not changed significantly during 2007–2016. By contrast, suspended sediment concentration at QXC and WX stations declined substantially with the trend terms decreasing at more than 1.00%/month (1.48%/month at QXC and 2.07%/month at WX). The decreasing trend term of suspended sediment concentration gradually increased at QXC and decreased at WX, suggesting suspended sediment at WX had been compensated by those on the channel bed from QXC to WX. The seasonal variations of water discharge and suspended sediment concentration during 2007–2016 were narrowed by 43.50% and 69.89%, respectively (Figures 2c and 2d). that is, the peaks in flood seasons declined, while the troughs in dry seasons increased, which shows a homogenization trend of the intra-year distribution.

4.2. Calibration and Validation of the Numerical Models

Here we used the data of QXC and WX stations (Figure 1) to calibrate the water flow model, suspended sediment model, and nitrogen cycle model, because there are no other stations for both hydrological observation and water quality monitoring between these locations. Considering the fact that the one-dimensional model that we applied is rather simple and does not have many parameters to calibrate, it should be acceptable to calibrate the model with the currently available data. Similar calibration of one-dimensional model has been common in previous research (e.g., Nittrouer & Viparelli, 2014), which shows the advantages of the one-dimensional model, that is,

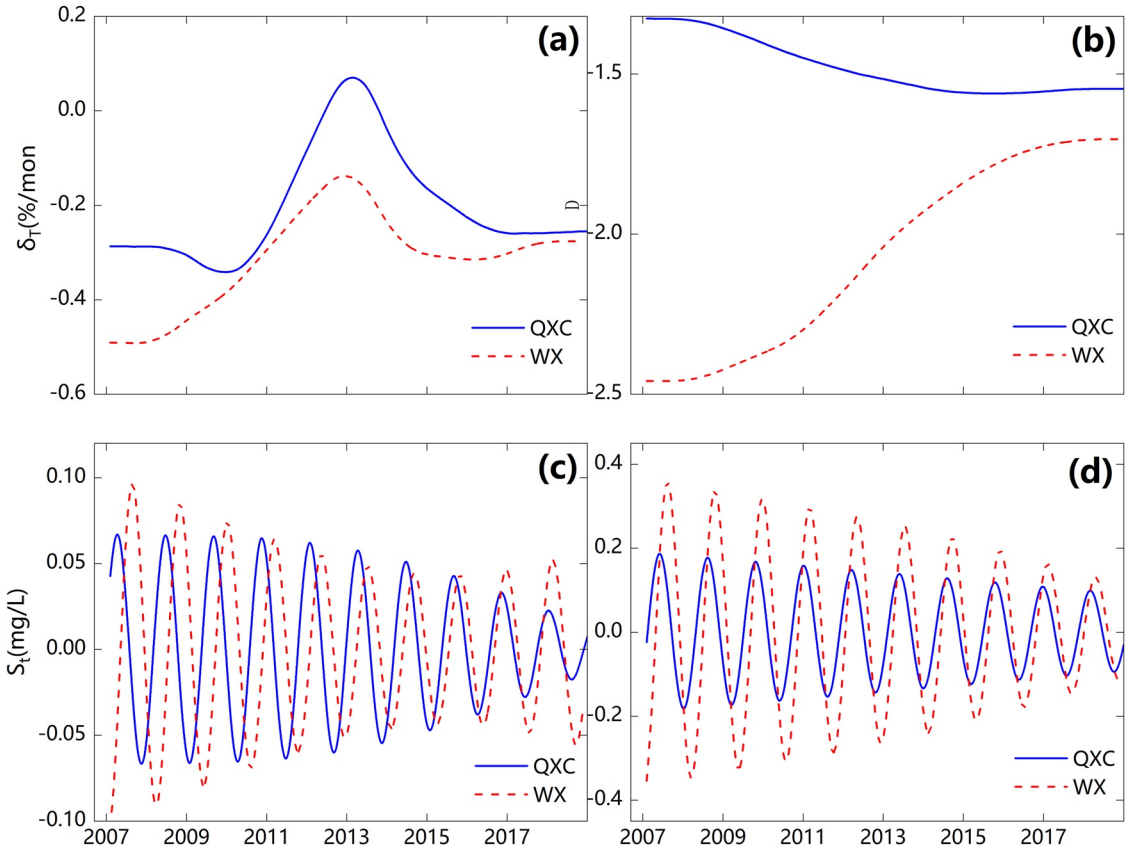

Figure 2. Trend coefficients (δ_T) for (a) flow quantity (Q) and (b) sediment concentration (S), and seasonal coefficients (S_t) for (c) flow quantity (Q) and (d) sediment concentration (S) at Qingxichang and Wanxian stations.

it well describes the broad scale characteristics of rivers after relatively simple calibration of a few parameters with much less data.

The Manning roughness of QXC and WX (Figure 1) were calibrated to be 0.0291 and 0.0473, respectively, based on genetic algorithm, very close to the results in Qi and Zhang (2019) (Figures S2a, S2b, and S2c in Supporting Information S1). Sediment transport capacity coefficient (k) and exponent (m) were derived as 0.20 and 0.92, respectively, consistent with the values for the TGR area in Yu et al. (2010) (Figure S2d in Supporting Information S1). Calibration of NH_3-N model was carried out at three NH_3-N concentration load levels, that is, high, medium, and low at WX (Table S2 in Supporting Information S1). The best fitted results were obtained at high-level (Figure S3a in Supporting Information S1), with the parameters of p_1, p_2, w_{af}, w_{an}, and w_{ad} being calibrated as 1.9147, 0.2772, 51.90%, 24.18%, and 23.92%. Similarly, the best fitted calibration results of TN model were found at high-level TN load (Figure S3b in Supporting Information S1), with p_3, p_4, w_{af}, w_{an}, and w_{ad} being calibrated as 9.8830, 0.3217, 36.76%, 36.43%, and 26.81%. Thus, the denitrification coefficient R_{N2} in Equation 10 was calculated in the range from 9.76 mg/m^2/d to 10.53 mg/m^2/d, much bigger than that (5.17 mg/m^2/d) obtained by Xia et al. (2017), mainly due to the difference between the real water environment in this study and the lab environment in Xia et al.'s study. It should be noted that most of NH_3-N and TN loads were allocated in flood seasons, possibly because large runoff in flood season leads to heavy runoff-washed NH_3-N loads from farmlands which are the major source for contamination in the TGR (Li & Huang, 2006).

Data of water level, suspended sediment concentration, and nitrogen concentrations at QXC and WX in 2011 were used for model validation. As shown in Table 1, the maximum absolute error of water level was within 1 m and the

Table 1
Validation Results for Hydrodynamic Model From 2011 to 2013[a]

	Water level	Flow	NH_3-N	TN
MAE[a]	0.609 m	–	–	–
ARE[b]	–	9.27%	–	–
RMSE[c]	0.107 m	1,429 m^3/s	0.0812 mg/L	0.1560 mg/L
MNE[d]	−0.080	0.229		

[a]MAE stands for maximum absolute error. [b]ARE represents average relative error. [c]RMSE is the root mean square error. [d]MNE is the abbreviation for modified nash-sutcliffe efficiency.

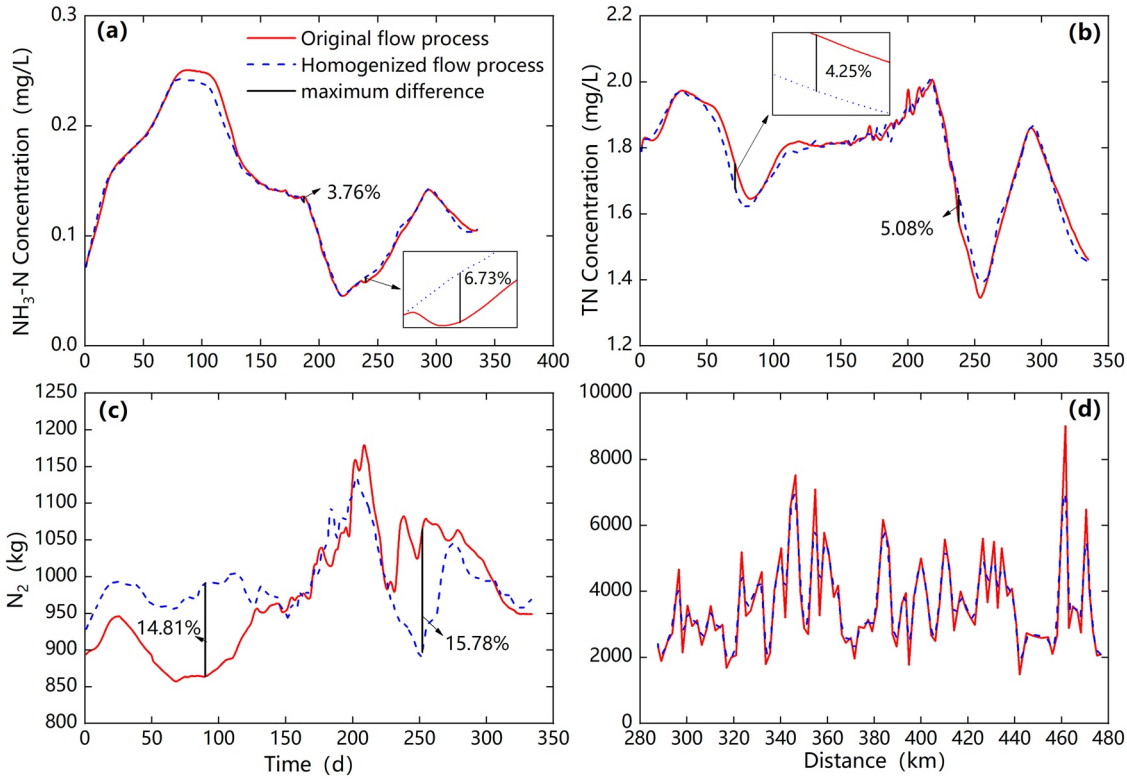

Figure 3. Comparison between the original flow process in 2010 and the homogenized flow process in 2016 for the temporal changes of (a) ammonia nitrogen (NH_3-N) concentration, (b) total nitrogen (TN) concentration, and (c) N_2 emission rate, and for the spatial distribution of (d) N_2 emission rate. Bars in (a), (b) and (c) show the maximum differences in flood and dry seasons in percentage.

average relative error was less than 10%; the values of Root Mean Square Error (RMSE) of water level and flow were all very small, suggesting a good performance of the water flow and suspended sediment transport model in this study. Despite that the Modified Nash-Sutcliffe Efficiencies (MNE) of NH3-N was slightly negative, the RMSEs of NH3-N and TN were very small, which implied that simulation of nitrogenous concentration might also be acceptable (Figures S4, S5, and Table S3 in Supporting Information S1).

The effects of sediment concentration change on nitrogen cycle have been incorporated (Equations 9 and 10) in this study, which is the major difference with models in previous studies. To further analyze the reasonability of the modified model, we compared the simulation results with and without such effects. The results showed that model without consideration of the sediments' effects had less desirable MNE (decreased by 15.0%) and RMSE (increased by 3%–12%), that is, the modified model in this study had better performance.

4.3. Effects of Homogenized Water Inflow on Nitrogen Cycle

To simulate the effect of homogenized water inflow on nitrogen cycle, we used flow process in 2016 (the ratio of annual flow in the flood season was 53.43%) to compare with that in 2010 (the ratio was 64.87%) at QXC station. Since no significant change (<2%) occurred between annual average flow in 2010 and 2016, the comparison was reasonable. As illustrated in Figure 3a, the highest increment of NH_3-N concentration was obtained in the non-flood season (6.73%), and the largest decrease occurred in the flood season by 3.76%. As the homogenization of water flow, nitrogen input from NH_3-N load of the upstream and of the lateral flows increases in the non-flood season and decreases in the flood season, which explained the rises and downs in NH_3-N concentration in TGR.

Figure 3b shows that TN concentration maximumly decreased by 4.25% in the non-flood season, while in the flood season the highest increment was 5.08%. Since TN concentration was much higher at WX than at QXC, exogenous TN load from lateral inflows was likely to be the major sources of TN in the TGR. And the reason for

the increase of TN in the non-flood season and decrease in the flood season under water flow homogenization was similar to that for NH_3-N.

Annual total N_2 gas emission did not change much (only increased by 1.59%). However, the seasonal N_2 release had been affected more significantly by flow homogenization. N_2 gas emission decreased by 14.81% in the flood season at maximum, while it increased most obviously by 15.78% in the non-flood season (Figure 3c). In other words, N_2 gas release varied more violently, with the variation range enlarged by 30%, confirming that nitrogen metabolism in aquatic environment is highly restrained by water flow conditions. In contrast, the spatial distribution of N_2 gas emission was not obviously affected by homogenization, as depicted in Figure 3d.

4.4. Effects of Sharply Reduced Sediment Concentration on Nitrogen Cycle

Since suspended sediment concentration in 2016 only accounted for 25% of that in 2010, we simulated the scenario that sediment concentration sharply reduced by 75%. According to Equations 9 and 10, nitrification and denitrification rates, K_0 and R_{N2}, also reduced by 32.3% and 7.2% with the decrease of sediment concentration (Figure 4).

The inhibited nitrification further led to NH_3-N accumulation, and the maximum increment was 4.87% (Figure 5a). Stronger influence on NH_3-N was found in dry and normal seasons rather than the flood seasons. In contrast, TN concentration was not significantly affected (Figure 5b), even though N_2 gas emission was reduced from 325.52 t/yr to 302.76 t/yr (6.99% of total N_2 gas emission) due to the decreased denitrification rate (Figure 5c). This was possibly because TN concentration in the studied area was very high, and N_2 gas emission took off a very small part from TN. Spatial distribution of N_2 gas emission (Figure 5d) showed that the maximum decline was 7.15%, due to both sediment reduction and the sharply narrowed section water surface area which is due to the terribly undulated topography along the reach.

Previous nitrogen models in natural water bodies seldom considered the effects of sediment concentration change on nitrogen cycle. Here we further compared the simulation results with and without such effects. The results showed that model without consideration of the sediments' effects simulated smaller NH_3-N and TN concentrations (by 18.84% and 3.38%, respectively, Figure S6a and S6b in Supporting Information S1) and greater N_2 gas emission rate (by 3.79%–13.79%, Figure S6c and S6d in Supporting Information S1). It implied that the severity of nitrogen pollution might be underestimated if the impacts of sediment concentration variations on nitrification/denitrification rates were not properly considered.

5. Discussion

5.1. Stability of Nitrogen Cycle and Implications for Aquatic Health

Simulation results of the nitrogen cycle (Figures 4a, 4b, 5a, and 5b) showed that the overall annual processes of NH_3-N and TN concentrations in TGR did not change much, implying that the nitrogen cycle basically remained stable in spite of drastic changes in water and sediment inflows, and thus, reducing the potential environmental risk brought by fierce fluctuation of nitrogenous substances concentrations. On the other hand, steady processes of NH_3-N and TN concentrations in the TGR also indicated a relatively stable microbial community in the water body and in the sediment (Geng et al., 2022), as similar phenomenon had occurred in soils (Zhu et al., 2021). Since the diversity of microbial community in water and sediments is usually considered as a potential bio-indicator to ecosystem health and to the degree of human perturbation (Newsome & Falagán, 2021; Wang et al., 2022), this relatively stable microbial community might suggest that aquatic environmental health did not deteriorate (Dzoga et al., 2018; Wang et al., 2022).

The N_2 emission was highly sensitive to the changes of water and suspended sediments (Figures 4d and 5d), implying flow condition and suspended sediment might be the main influencers to N_2 producing processes, including denitrification and anaerobic ammonia oxidation (Liu et al., 2013; Zhang et al., 2020). The violently changed N_2 emission rates also indicated a quick response and relatively strong adaptation of microbial N_2 producing processes (Dzoga et al., 2018). As Dzoga et al. (2018) suggested that adaptation is usually regarded as another environmental health indicator which has a positive relationship with ecosystem robustness (Dzoga et al., 2018), ecological functions related to nitrogen cycling could possibly be maintained in TGR under water and sediment changes.

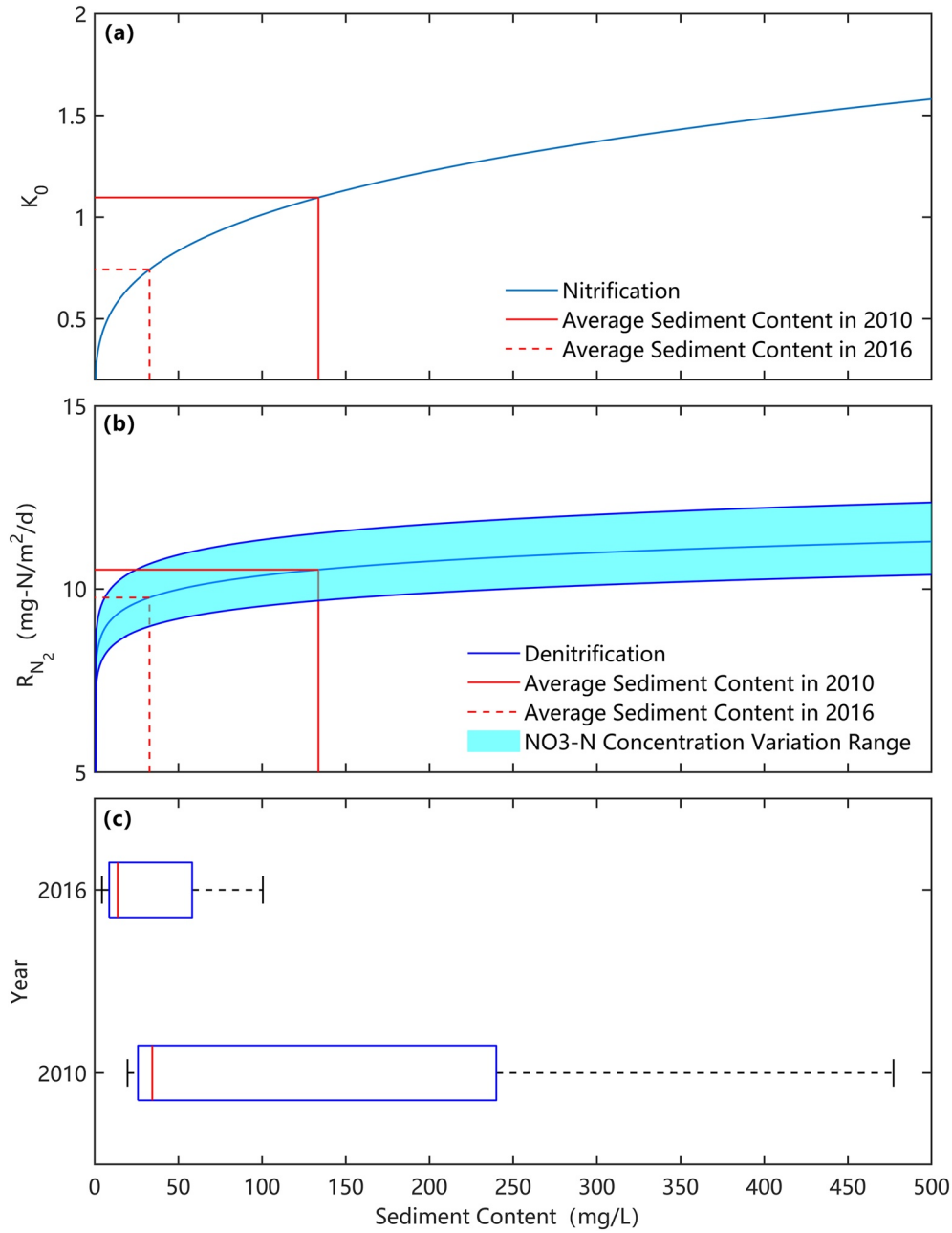

Figure 4. Effects of sediment concentration on (a) nitrification and (c) denitrification processes with (c) box diagram of sediment concentration (K_0 is the coefficient presenting the effect of sediment concentration on nitrification; R_{N2} is N_2 gas release rate).

5.2. Model Sensitivity and Limitations

Here we tested the sensitivity of the model parameters to analyze the uncertainties of parameterizing. Changing the Manning roughness (n), sediment transport capacity coefficient (k) and exponent (m), and parameters in Equations 9 and 10 (i.e., p_1, p_2, w_{af}, w_{an}, w_{ad} and p_3, p_4, w_{af}, w_{an}, w_{ad}) by ±30%, ±20%, and ±10%, it showed in Table 2 that variations of water level, discharge and sediment concentration were all less than 0.5%, indicating that the water flow and sediment transport models are very robust. The variation ranges of NH_3-N and TN were also smaller than the changing ranges of parameters (Table 2). However, N_2 emission rates could be very sensitive, possibly because N_2 is not the only endpoint of denitrification processes in reality, which is against the model assumption, implying large uncertainty in the simulation of N_2 emission. Moreover, the accurate dissolved N_2

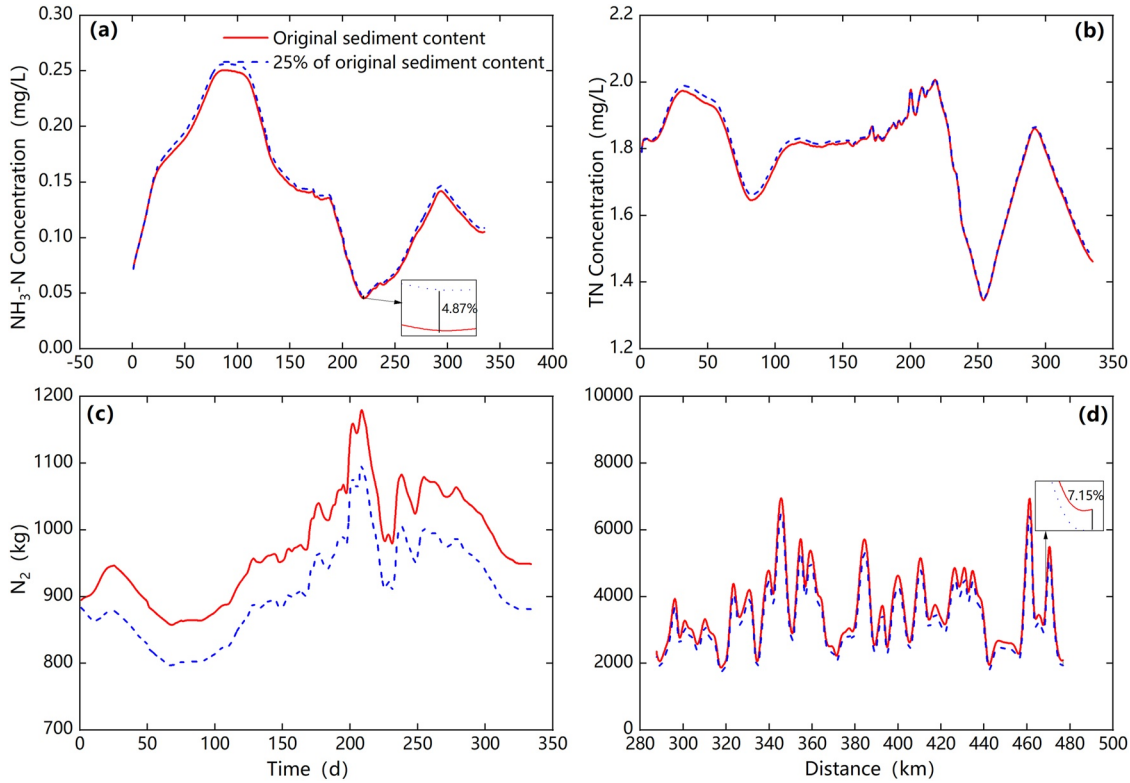

Figure 5. Comparison between the original sediment concentration process in 2010 and the sharply decreased sediment concentration process in 2016 for the temporal changes of (a) ammonia nitrogen (NH_3-N) concentration, (b) total nitrogen (TN) concentration, and (c) N_2 emission rate, and for the spatial distribution of (d) N_2 emission rate. Bars in (a) and (c) show the maximum differences in percentage.

concentration and the real N_2 emission rate have not been measured using the ^{15}N tracers or $\delta^{15}N$ assays method, which is also a limitation of this study. Considering that gas emissions during nitrogen cycle exert important effects on both aquatic environment and global warming, deep investigation should be carried out to reveal the detailed processes and mechanisms, based on which the model can be further improved. Besides, it should be noted that ecosystem health is affected by various natural and anthropogenic factors. Thus, comprehensive investigation on more factors acting on microbial function and ecological stability is still needed in future studies.

Limitations of model simulation in this study were mainly due to certain model assumption and inadequacy of data. The model assumptions that intra-annual distribution of exogenous loads maintains over the whole study period and N_2 was the only gaseous production during the nitrogen cycle were too ideal. As to the data sources, measured underwater topographic data of the TGR in 2003 was used to represent the whole study period, without consideration of sedimentation in the backwater area after 2003. The predicted loads by Li and Huang (2006) applied as exogenous load in this study has been proved to be 15.6% higher than the actual ones in 2010 at the low-level scenario of NH_3-N. Furthermore, hydrological gauging stations and water quality observation stations are very sparse for model calibration. Therefore, further efforts to improve the model and the input data quality are highly encouraged.

Table 2
The Results Under Different Variation of Aquatic Health Indicators

Percentage of parameter variation (%)	ΔZ (%)	Δq (%)	ΔS (%)	NH_3-N (%) Maximum variation range	TN (%) Maximum variation range	N_2 (%) Maximum variation range
30	0.30	0.00	−0.27	−5.03	−15.86	61.07
−30	−0.26	0.00	0.29	5.73	8.11	−20.47
20	0.20	0.00	−0.19	−3.41	−11.76	46.53
−20	−0.18	0.00	0.20	3.70	4.23	−7.80
10	0.10	0.00	−0.09	−1.74	−7.70	32.38
−10	−0.09	0.00	0.10	1.82	−2.12	5.23

6. Conclusion

The influence of dramatically changed water and suspended sediment inflows in the TGR on aquatic nitrogen cycling in the reservoir area was investigated by the combined approach of DHR analysis and numerical models

which incorporated the effects of sediment concentration variations on nitrification/denitrification processes, using long-time sequenced data collected at QXC and WX stations. The flattened intra-year distribution of water inflow and dramatically reduced suspended sediment concentration were obtained. However, yearly processes of NH_3-N and TN concentrations remained relatively stable, reflecting the stability of microbial community related to nitrogen cycle. In contrast, changes in N_2 emission were more violently under significantly changed water and sediment inflows. Additionally, the reduced N_2 emission in the simulation for sediment reduction might be a positive sign for a relieved pressure on nitrogen oxide control. However, since we assumed N_2 was the only endpoint of nitrification, emissions of other nitrogenous gases still need to be quantified in future studies.

Conflict of Interest

The authors declare no conflicts of interest relevant to this study.

Data Availability Statement

Data of water flow, suspended sediment concentration, ammonia nitrogen concentration and total nitrogen concentration are provided by the Bureau of Hydrology, Changjiang Water Resources Commission, China, and available at Zenodo via https://doi.org/10.5281/zenodo.6801085 (Yue, 2022).

Acknowledgments
This study has been supported by the Open Fund for the State Key Laboratory of Water Resources and Hydropower Engineering Science, Wuhan University (Grant No. 2019HLG01), the National Key R&D Program of China (Grant No. 2016YFA0600901), and the National Natural Science Foundation of China (Grant No. 52079094). The authors also gratefully acknowledge the contributions of the Changjiang Water Resources Commission for providing access to the unique research data set.

References

Abdul-Aziz, O. I., & Ahmed, S. (2017). Relative linkages of stream water quality and environmental health with the land use and hydrologic drivers in the coastal-urban watersheds of southeast Florida. *GeoHealth*, *1*(4), 180–195. https://doi.org/10.1002/2017GH000058

An, C., Moodie, A. J., Ma, H., Fu, X., Zhang, Y., Naito, K., & Parker, G. (2018). Morphodynamic model of the lower Yellow River: Flux or entrainment form for sediment mass conservation? *Earth Surface Dynamics*, *6*(4), 989–1010. https://doi.org/10.5194/esurf-6-989-2018

APHA (American Public Health Association), AWWA (American Water Works Association), WEF (Water Environment Federation). (2012). *Standard methods for the examination of water and wastewater*. American Public Health Association.

Chai, Y., Yue, Y., Zhang, L., Miao, C. Y., Borthwick, A. G. L., Zhu, B. Y., et al. (2020). Homogenization and polarization of the seasonal water discharge of global rivers in response to climatic and anthropogenic effects. *Science of the Total Environment*, *709*, 136062. https://doi.org/10.1016/j.scitotenv.2019.136062

Deng, C. G. (2007). *Research on eutrophication in the three Gorges reservoir area*. China Environmental Science Press. (in Chinese).

Dzoga, M., Simatele, D., & Munga, C. (2018). Assessment of ecological vulnerability to climate variability on coastal fishing communities: A study of Ungwana Bay and Lower Tana Estuary, Kenya. *Ocean & Coastal Management*, *163*, 437–444. https://doi.org/10.1016/j.ocecoaman.2018.07.015

GB3838-2002. (2002). *Environmental quality standards for surface water*. State Environmental Protection Administration, the People's Republic of China. (in Chinese).

Geng, M. D., Zhang, W. Z., Hu, T., Wang, R., Wang, J. J., & Cheng, X. Y. (2022). Eutrophication causes microbial community homogenization via modulating generalist species. *Water Research*, *210*, 118003. https://doi.org/10.1016/j.watres.2021.118003

Gu, C. Y. (2005). *Study on the steady-state water quality model in Chongqing section of the three Gorges reservoir area* (master's thesis), (in Chinese). Chongqing University. Retrieved from https://kns.cnki.net/kcms/detail/detail.aspx?dbcode=CMFD&dbname=CMFD2007&filename=2006054814.nh&uniplatform=NZKPT&v=Ele0pqVbDIDbAoTGjH83fbXBgKSSR88B3qzXPPIpc_L_JUrZ5LkCq5sMwxBC2LZg

Guo, L. C., Wegen, M. V. D., Wang, Z. B., Roelvink, D., & He, Q. (2016). Exploring the impacts of multiple tidal constituents and varying river flow on long-term, large-scale estuarine morphodynamics by means of a 1-D model. *Journal of Geophysical Research: Earth Surface*, *121*(5), 1000–1022. https://doi.org/10.1002/2016JF003821

HJ535-2009. (2009). *Water quality-Determination of ammonia nitrogen-Nessler's reagent spectrophotometry*. Ministry of Environmental Protection, the People's Republic of China. (in Chinese).

Knoll, A. H., Canfield, D. E., & Konhauser, K. O. (2012). *Fundamentals of geobiology* (pp. 36–48). John Wiley & Sons, Inc.

Li, C. M., & Huang, Z. L. (2006). Study on inflow pollution load of Three Gorges Reservoir (II)–Prediction of pollution load after impounding. *Resources and Environment in the Yangtze Basin*, *15*, 97–106. (in Chinese).

Li, L., Ni, J. R., Chang, F., Yue, Y., Frolova, N., Magritsky, D., et al. (2020). Global trends in water and sediment fluxes of the world's large rivers. *Science Bulletin*, *65*(1), 62–69. https://doi.org/10.1016/j.scib.2019.09.012

Liu, C. Y., Wang, Y. T., Zhou, J. Q., Chen, Y. Z., Zhou, J., Wang, Y. Y., & Fu, D. F. (2021). Migration and transformation of nitrogen in sediment–water system within storm sewers. *Journal of Environmental Management*, *287*, 112355. https://doi.org/10.1016/j.jenvman.2021.112355

Liu, F. B., Feyen, J., & Berlamont, J. (1994). Downstream control algorithm for irrigation canals. *Journal of Irrigation and Drainage Engineering*, *120*(3), 468–483. https://doi.org/10.1061/(asce)0733-9437(1994)120:3(468)

Liu, T., Xia, X. H., Liu, S. D., Mou, X. L., & Qiu, Y. W. (2013). Acceleration of denitrification in turbid rivers due to denitrification occurring on suspended sediment in oxic waters. *Environmental Science & Technology*, *47*(9), 4053–4061. https://doi.org/10.1021/es304504m

Newsome, L., & Falagán, C. (2021). The microbiology of metal mine waste: Bioremediation applications and implications for planetary health. *Geohealth*, *5*(10), 2020GH000380. https://doi.org/10.1029/2020GH000380

Nittrouer, J. A., & Viparelli, E. (2014). Sand as a stable and sustainable resource for nourishing the Mississippi River delta. *Nature Geoscience*, *7*(5), 350–354. https://doi.org/10.1038/ngeo2142

Qi, M. J., & Zhang, X. F. (2019). Selection of appropriate topographic data for 1D hydraulic models based on impact of morphometric variables on hydrologic process. *Journal of Hydrology*, *571*, 585–592. https://doi.org/10.1016/j.jhydrol.2018.10.079

Quick, A. M., Reeder, W. J., Farrell, T. B., Tonina, D., Feris, K. P., & Benner, S. G. (2019). Nitrous oxide from streams and rivers: A review of primary biogeochemical pathways and environmental variables. *Earth-Science Reviews*, *191*, 224–262. https://doi.org/10.1016/j.earscirev.2019.02.021

Ran, X. B., Bouwman, L., Yu, Z. G., Beusen, A., Chen, H. T., & Yao, Q. Z. (2017). Nitrogen transport, transformation, and retention in the Three Gorges Reservoir: A mass balance approach. *Limnology & Oceanography*, *62*(5), 2323–2337. https://doi.org/10.1002/lno.10568

Reaver, K. M., Levy, J., Nyambe, I., Hay, M. C., Mutiti, S., Chandipo, R., & Meiman, J. (2021). Drinking water quality and provision in six low-income, peri-urban communities of Lusaka, Zambia. *GeoHealth*, *5*(1), e2020GH000283. https://doi.org/10.1029/2020GH000283

Schrag, J. M. (2017). Naturally occurring radium (Ra) in home drinking-water wells in the Sandhills region of South Carolina, USA: Can high concentrations be predicted? *GeoHealth*, *1*(4), 138–150. https://doi.org/10.1002/2017GH000069

SL219-2013. (2013). *Regulation for water environmental monitoring*. Ministry of Water Resources, the People's Republic of China. (in Chinese).

Taylor, C. J., Pedregal, D. J., Young, P. C., & Tych, W. (2007). Environmental time series analysis and forecasting with the Captain toolbox. *Environmental Modelling & Software*, *22*(6), 797–814. https://doi.org/10.1016/j.envsoft.2006.03.002

Tong, Y. D., Bu, X. G., Chen, J. Y., Zhou, F., Chen, L., Liu, M. D., et al. (2017). Estimation of nutrient discharge from the Yangtze River to the East China Sea and the identification of nutrient sources. *Journal of Hazardous Materials*, *321*, 728–736. https://doi.org/10.1016/j.jhazmat.2016.09.011

Wang, H., Liu, S. E., Li, H. Y., Tao, X. H., Wang, H. C., Qi, J. F., & Zhang, Z. J. (2022). Large-scale homogenization of soil bacterial communities in response to agricultural practices in paddy fields, China. *Soil Biology and Biochemistry*, *164*, 108490. https://doi.org/10.1016/j.soilbio.2021.108490

Wang, H. Y., Shen, Z. Y., Guo, X. J., Niu, J. F., & Kang, B. (2010). Ammonia adsorption and nitritation in sediments derived from the Three Gorges Reservoir, China. *Environmental Earth Sciences*, *60*(8), 1653–1660. https://doi.org/10.1007/s12665-009-0299-7

Widdig, M., Heintz-Buschart, A., Schleuss, P. M., Guhr, A., Spohn, M., & Seabloom, E. W. (2020). Effects of nitrogen and phosphorus addition on microbial community composition and element cycling in a grassland soil. *Soil Biology and Biochemistry*, *151*, 108041. https://doi.org/10.1016/j.soilbio.2020.108041

Xia, X., Liu, T., Yang, Z., Michalski, G., Liu, S. D., Jia, Z. M., & Zhang, S. B. (2017). Enhanced nitrogen loss from rivers through coupled nitrification-denitrification caused by suspended sediment. *Science of the Total Environment*, *579*, 47–59. https://doi.org/10.1016/j.scitotenv.2016.10.181

Xia, X. H., Li, S. Z., & Shen, Z. Y. (2008). Effect of nitrification on nitrogen flux across sediment-water interface. *Water Environment Research*, *80*(11), 2175–2182. https://doi.org/10.2175/106143008X296505

Ylla Arbós, C., Blom, A., Viparelli, E., Reneerkens, M., Frings, R. M., & Schielen, R. M. J. (2021). River response to anthropogenic modification: Channel steepening and gravel front fading in an incising river. *Geophysical Research Letters*, *48*(4), e2020GL091338. https://doi.org/10.1029/2020GL091338

Yu, J. H., Fan, C. X., Zhong, J. C., Zhang, L., Zhang, L., Wang, C. H., & Yao, X. L. (2016). Effects of sediment dredging on nitrogen cycling in Lake Taihu, China: Insight from mass balance based on a 2-year field study. *Environmental Science and Pollution Research*, *23*(4), 3871–3883. https://doi.org/10.1007/s11356-015-5517-0

Yu, J. H., Zhang, Y. S., Zhong, J. C., Ding, H., Zheng, X. Z., Wang, Z. Y., & Zhang, Y. L. (2019). Water-level alterations modified nitrogen cycling across sediment-water interface in the three gorges reservoir. *Environmental Science and Pollution Research*, *27*(21), 25886–25898. https://doi.org/10.1007/s11356-019-06656-z

Yu, X. Z., Liao, W. G., & Lu, P. Y. (2010). *Effects of sediment on major pollutants in the Three Gorges Reservoir area*. Science Press. (in Chinese).

Yue, Y. (2022). Water, sediment and nitrogen data of Qingxichang and Wanxian, China [Data set]. Zenodo. https://doi.org/10.5281/zenodo.6801085

Zhang, R. J. (1998). *Dynamics of river sediment* (2nd ed.). China WaterPower Press. (in Chinese).

Zhang, W. L., Shi, M., Wang, L. Q., Li, Y., Wang, G. L., Niu, L. H., et al. (2021). New insights into nitrogen removal potential in urban river by revealing the importance of microbial community succession on suspended particulate matter. *Environmental Research*, *204*, 112371. https://doi.org/10.1016/j.envres.2021.112371

Zhang, X., Ward, B. B., & Sigman, D. M. (2020). Global nitrogen cycle: Critical enzymes, organisms, and processes for nitrogen budgets and dynamics. *Chemical Reviews*, *120*(12), 5308–5351. https://doi.org/10.1021/acs.chemrev.9b00613

Zhang, X. F., Yan, H. C., Yue, Y., & Xu, Q. X. (2019). Quantifying natural and anthropogenic impacts on runoff and sediment load: An investigation on the middle and lower reaches of the Jinsha River Basin. *Journal of Hydrology: Regional Studies*, *25*, 100617. https://doi.org/10.1016/j.ejrh.2019.100617

Zhao, Y. Y., Zheng, B. H., Jia, H. F., & Chen, Z. X. (2019). Determination sources of nitrates into the three gorges reservoir using nitrogen and oxygen isotopes. *Science of the Total Environment*, *687*, 128–136. https://doi.org/10.1016/j.scitotenv.2019.06.073

Zhu, X. H., Zhang, L. H., Zuo, Y. J., Liu, J. Z., Yu, J. L., Yuan, F. H., et al. (2021). Wetland reclamation homogenizes microbial properties along soil profiles. *Geoderma*, *395*(5), 115075. https://doi.org/10.1016/j.geoderma.2021.115075